Large area and low power dielectrowetting optical shutter with local deterministic fluid film breakup

R. Zhao,[1,2] B. Cumby,[1] A. Russell,[1] and J. Heikenfeld[1,a)]
[1]*Novel Devices Laboratory, Department of Electrical Engineering and Computing Systems, University of Cincinnati, Cincinnati, Ohio 45221, USA*
[2]*Center of Optofluidic Technology, College of Optoelectronic Engineering, Nanjing University of Posts and Telecommunications, Nanjing, Jiangsu 210003, China*

(Received 30 July 2013; accepted 7 November 2013; published online 27 November 2013; publisher error corrected 2 December 2013)

A large area (>10 cm^2) and low-power (0.1–10 Hz AC voltage, ~10's $\mu W/cm^2$) dielectrowetting optical shutter requiring no pixelation is demonstrated. The device consists of 40 μm interdigitated electrodes covered by fluid splitting features and a hydrophobic fluoropolymer. When voltage is removed, the fluid splitting features initiate breakup of the fluid film into small droplets resulting in ~80% transmission. Both the dielectrowetting and fluid splitting follow theory, allowing prediction of alternate designs and further improved performance. Advantages include scalability, optical polarization independence, high contrast ratio, fast response, and simple construction, which could be of use in switchable windows or transparent digital signage. © *2013 AIP Publishing LLC*. [http://dx.doi.org/10.1063/1.4834095]

Highly optically efficient shutters remain a significant challenge, despite the large number of technologies that have been developed for transmissive and reflective displays.[1–3] Some applications, such as smart windows or switchable architectural/privacy glass, pose even greater challenges, including a need for very low cost, low haze, default to a clear state with power-failure and a desire for optical transparencies that are beyond the <50%, typical of existing commercial products. Current approaches for smart windows include[4–13] photoelectrochromics, photochromics, thermotropic, polymer-dispersed liquid crystal, thermochromics, suspended particle, electrochromics, counterion exchange, and electrowetting. For large area windows or architectural glass, unlike pixelated (matrix) displays, one aspect that is not highly constrained is the use of higher voltage or frequency as long as the power consumption is adequately low (high voltage/frequency inverters are low cost, e.g., compact fluorescent bulbs). Recently, with an AC voltage of ~200 to 300 Vpp and voltage frequency of 10 kHz, superspreading of fluids has been demonstrated by dielectrowetting.[14,15] The term dielectrowetting is utilized because the underlying wetting effect is driven by dielectrophoresis[16] (nonuniform electric fields, electrically insulating fluid) and because the cosine of the contact angle follows a voltage-squared wetting dependence similar to conventional electrowetting[17,18] (electrically conducting fluid). Similar dielectrophoretic or electrowetting modulation has also been recently used for tunable-focus microlenses,[19,20] color displays,[21] and optical switches.[22,23] Here, we demonstrate dielectrowetting superspreading and deterministic dewetting of an opaque ink fluid to create an ultra-simple and large-area (>10 cm^2) optical shutter which operates at very low power (~10's $\mu W/cm^2$ at 0.1–10 Hz AC voltage). The ink is wetted from numerous sessile droplets into a continuous and optically opaque ~15 μm thick film (T < 1.5% ~ 420–680 nm). When voltage is removed, the fluid splitting features then rapidly (100's ms) and deterministically initiate breakup of the ink back into small sessile droplets, resulting in a very high 80% optical transmission with very low haze. Both the dielectrowetting superspreading and the ink film breakup closely follow expected theoretical behavior. The applications for this device include those desirable of large sizes, high optical clarity, clear appearance with power failure, independence of polarization or angle, very high contrast ratio (average ~400:1 for several portions of the visible spectrum), fast response, and simple low cost fabrication, all of which are valuable for applications in smart windows, switchable architectural glass, or transparent or reflective digital signage.

Figure 1 shows an operating diagram of the dielectrowetting optical shutter. A brief description of the device structure, materials, and fabrication is now provided, and more detailed description, including experimental procedures, is provided in the supplementary material.[24] As shown in Figure 1(a) the device substrate has interdigitated ITO electrodes with 40 μm line width and gap spacing on 2 in. × 2 in. glass, without a superstrate (top plate). In practical applications, hermetic sealing with a superstrate would be required, but the top-plate if spaced with adequate distance from the substrate does not significantly affect the device physics discussed herein. Onto the substrate and electrodes, ~15 μm tall splitting features are fabricated by contact printing of any type of electrically insulating polymer, followed then by uniform solution coating with ~50 nm of a hydrophobic fluoropolymer film. The ink is an electrically insulating and high dielectric constant fluid (in this case liquid crystal, $\varepsilon \sim 35$) that is colored black with a blend of dyes. On the fluoropolymer, the ink has a Young's angle of $\theta \sim 80°$. When voltage is applied, non-uniform electric fields generated by the interdigitated electrodes exert a dielectrophoretic force (F) on the ink droplet[20]

$$F = \frac{1}{2}\varepsilon_0(\varepsilon_i - 1)\nabla E^2, \quad (1)$$

a)Author to whom correspondence should be addressed. Electronic mail: heikenjc@ucmail.uc.edu

 © 2013 AIP Publishing LLC

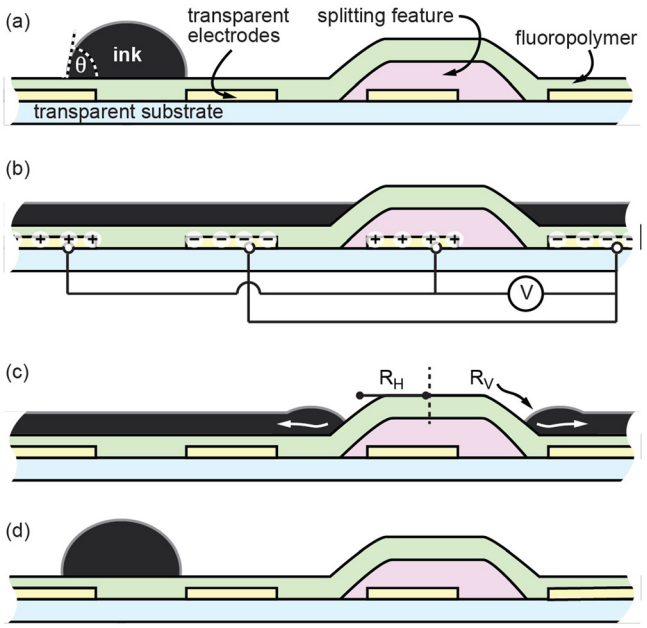


FIG. 1. Diagram of the dielectrowetting optical shutter and its operation (side view).

where ε_i is the dielectric constant of the ink and E denotes the electric field. The force can reduce the contact angle of the ink droplet (dielectrowetting), even to the point of superspreading.[14,15] Wetting down to a continuous fluid film is unique to dielectrowetting and comparably remarkable because with conventional electrowetting[2,17,18] the fluid wetting typically saturates at a contact angle of $\theta \sim 60$–$70°$.[25] In the superspreaded state, the opaque film of ink blocks the incident light and leads to a black state shown in Figure 1(b). If the polymer used for the splitting feature is also colored black with dye, light is completely blocked over the entire area of the device.

In initial trials without splitting features, when the voltage was removed, the ink film would dewet very slowly (several seconds) from its edges into a single or few droplets of visibly objectionable size (~1 cm) and of such a large droplet volume that gravity depressed the droplet height and increased the apparent size. Furthermore, with large droplets, only horizontal substrate operation was possible (else droplets would overcome wetting hysteresis and flow in the direction of gravity). Therefore, a mechanism to split the ink film into much smaller droplets was needed. The ink films are >10 μm in thickness, which is more than an order of magnitude greater than the thickness where van der Waals forces could cause more localized ink film breakup.[26] This significant drawback was resolved by the inclusion of splitting features (Fig. 1(c)). In this work, the splitting features locally lower the dielectrowetting force by having a thickness and dielectric constant which provides >10× less electrical capacitance than the ink film. Therefore, under applied voltage the continuous ink film must wet around, not over or covering, the splitting features. When the voltage is removed, the splitting features then provide a deterministic mechanism to nucleate the dewetting of the ink film from the hydrophobic fluoropolymer. This localized ink film breakup gives rise to several desirable aspects from an applied perspective: (1) localized breakup reduces the visible size of the resulting droplets as compared to the resulting droplet without splitting features; (2) these smaller dewetted droplets also eliminate the effect of gravity (allows vertical substrate operation); (3) the distance over which the fluid must wet or dewet is decreased and therefore increases the speed of actuation (both wetting and dewetting) by an order of magnitude or more. Importantly, operation with small-size ink droplets is achieved without need for precise pixelation[21] of the device. The deterministic nucleation of the ink film breakup does require a critical radius (R_c) for the splitting features (Figure 1(c)), which for a given film thickness h and contact angle θ is[26,27]

$$R_C = h/\tan\theta\left(\sqrt{1+\cos\theta}-1\right). \quad (2)$$

Using the value $h = 15\,\mu$m for the thickness of the ink film and $\theta < 20$ to 80° for contact angle (see results) predicts $R_c > 105$ to 25 μm. If ink splitting is attempted with a "hole" in the ink that is less than R_C then surface tension (Laplace pressure) will instead cause the ink to collapse the "hole" rather than expand it in size.[27] A range of angles is given above for two reasons. First, the contact angle is dynamic when voltage is first removed. Second, the splitting cannot be thought of only terms of receding ink because while voltage is applied the ink must also be kept from advancing over top of the splitting feature. Because of this second reason, the lower angle (and larger R_c) is likely most appropriate. Furthermore, the side-wall slope of the splitting feature matters (e.g., wetting into a corner geometry phenomena). Therefore, more advanced theory and optimization of the splitting features is needed and is reserved for future work. It should also be noted that the knowledge base for splitting of fluid films in other types of electrowetting devices is relevant to deeper theoretical understanding of this work.[28,29]

The operating principles of the device are photographically demonstrated over a large area sample in the time-lapse images of Figure 2. A video from which these time-lapse images are taken can be found in the supplementary material for device operation.[24] In this work, the splitting features were simply applied randomly by contact printing with sizes well above the minimum R_C. The average diameter of the splitting features was ~250 μm, and the average distance between splitting features was ~1200 μm. The photographs show superspreading of the ink film, generating an opaque optical shutter over most of the electrode area, with exception of the few line-outs that are due to fabrication defects. The ink film breakup is also clearly demonstrated, nucleated at the splitting features, and results in smaller ink droplets and high optical transparence in the zero voltage state. The sample is being held vertically.

Because of the highly insulating nature of the liquid crystal and because the dyes were substantially purified of electrically conductive contaminants,[30] devices were found to operate down to frequencies as low as 0.1 Hz AC voltage, well below the 10's kHz to MHz frequencies, and the high power consumption/joule-heating, used in conventional dielectrophoresis. Exact power consumption calculations are non-trivial due to the multi-faceted capacitance during operation. Preliminary calculations were made using a purely

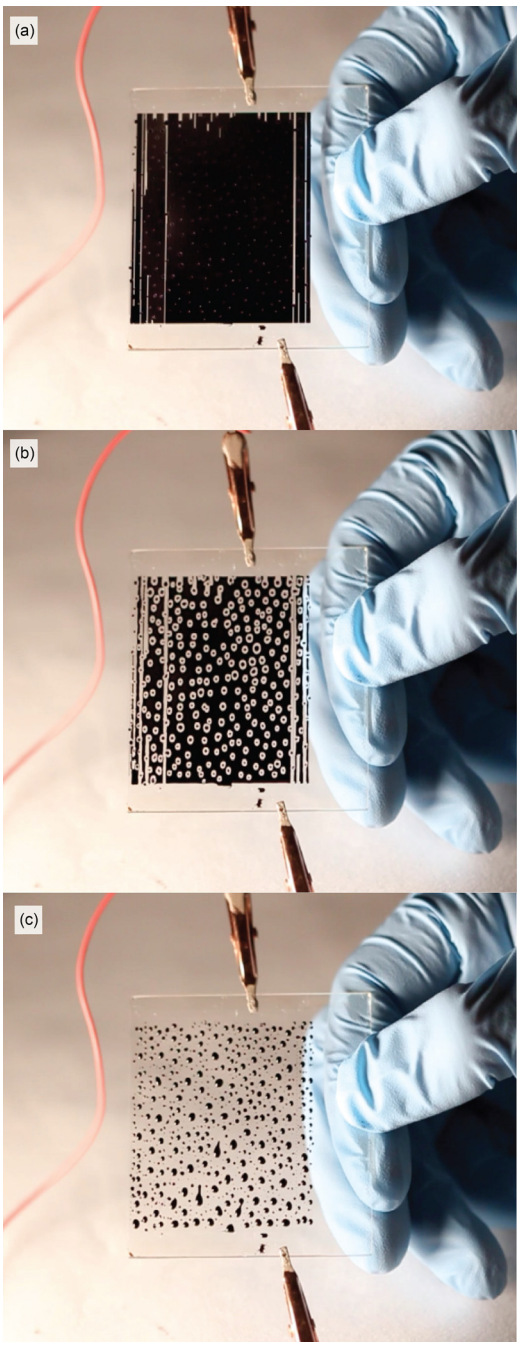


FIG. 2. Photos of the device operation: (a) t = 0, the opaque state (square wave, 10 Hz AC voltage, >200 Vpp); (b) the voltage removed at t = 0+ and a photograph taken at t = 167 ms showing the growth of holes in the ink film at splitting features; (c) t = 1700 ms and the dewetted equilibrium state with high optical transparency. Line-outs are simply due to a few fabrication defects over the large sample area (Multimedia view). [URL: http://dx.doi.org/10.1063/1.4834095.1]

electrical model developed elsewhere[31] and also based on surface energy of the fluid and the experimental contact angle range. Both of these calculations confirm that power consumption is on order of ~10's μW/cm^2 at 1 Hz AC voltage operation.

The wetting modulation was observed to be frequency independent except for two effects: (1) below 0.1 Hz even the liquid crystal was not adequately insulating to sustain the electric field that drives the dielectrowetting effect; (2) for frequencies of 10's Hz and below, a visible flickering of the superspread film could be seen, suggesting that the actual RMS voltage applied to the device is lower than the theoretically expected one due to the RC charging time of the device as voltage polarity switches for the AC square wave. Regarding this visual flickering, others have also shown more sophisticated "wrinkling" of a fluid/air interface[16] by dielectrophoresis to create effects such as tunable optical diffraction. DC voltages or lower-frequencies were not further pursued because it is well known that liquid crystal devices become damaged under long-term DC bias. Addressing aging is beyond the scope of this first report, but preliminary work was also performed by adding a ~1 μm Parylene C dielectric to prevent any net ion migration and electrode damage, and the device still operated down to 10 Hz AC voltage.

The contact angle response vs. voltage was also explored and is plotted in Figure 3 for 0.1, 1, and 10 Hz AC peak-to-peak voltage (Vpp). The data show θ decreasing down to 0°, representative of our measurement of continuous film, but the film itself forms in the range of 10° − 15° as is consistent with other work.[14,15] The plots reveal a similar response for frequencies in the range of 0.1–10 Hz AC voltage, all with low wetting hysteresis ($\Delta\theta < 10^\circ$) as the voltage is decreased back to zero. As stated previously, higher AC voltage frequencies of 100 and 1000 Hz were also tested and showed a similar response curve (not shown). Sinusoidal and other waveforms were applied, and similar behavior observed at equivalent root-mean-square voltages. The experimental contact angle results were plotted along with theoretical results using dielectrowetting theory provided by McHale *et al.*[14]

$$\cos\theta = \cos\theta_0 + \frac{\pi\varepsilon_0(\varepsilon_i - 1)}{8w\gamma_{lv}}(CV)^2,$$
$$C = \left(1 + \frac{\varepsilon_d - \varepsilon_i}{\varepsilon_d + \varepsilon_i}\right)e^{-\pi t_d/2w} \Big/ \left(1 + \left(\frac{\varepsilon_d - \varepsilon_i}{\varepsilon_d + \varepsilon_i}\right)e^{-\pi t_d/w}\right), \quad (3)$$

where ε_i is the dielectric constant of the ink, ε_d is the dielectric constant of the dielectric layer, t_d, is the thickness of the dielectric layer, w denotes the electrode width and gap spacing, and γ_{lv} is the liquid-vapor (air) interfacial surface tension of the ink. As plotted in Figure 4, the experimental results follow the theoretical results, with an expected deviation as the experimental results achieve the minimum physical wetting angle of a continuous ink film (cos 0° = 1). It is therefore reasonable to expect, if desired, achieving lower voltage operation by increased dielectric constant of the ink, reduced electrode width and spacing, and lower surface tension of the ink through surfactants or through replacing air with an oil to instead reduce interfacial surface tension.[21,23]

The spreading and dewetting time of the ink was also measured. The standard metric for an optical shutter is the transition time between 10% and 90% of the full optical transmission range. Figure 5 plots the ink area covering the substrate vs. time, which is closely predictive of transmission. The ink was found to spread more quickly (<500 ms) than it required to fully dewet (<1 s). If faster switching speeds are desired (<100 ms), the foremost methods for improvement include reducing ink viscosity (the liquid

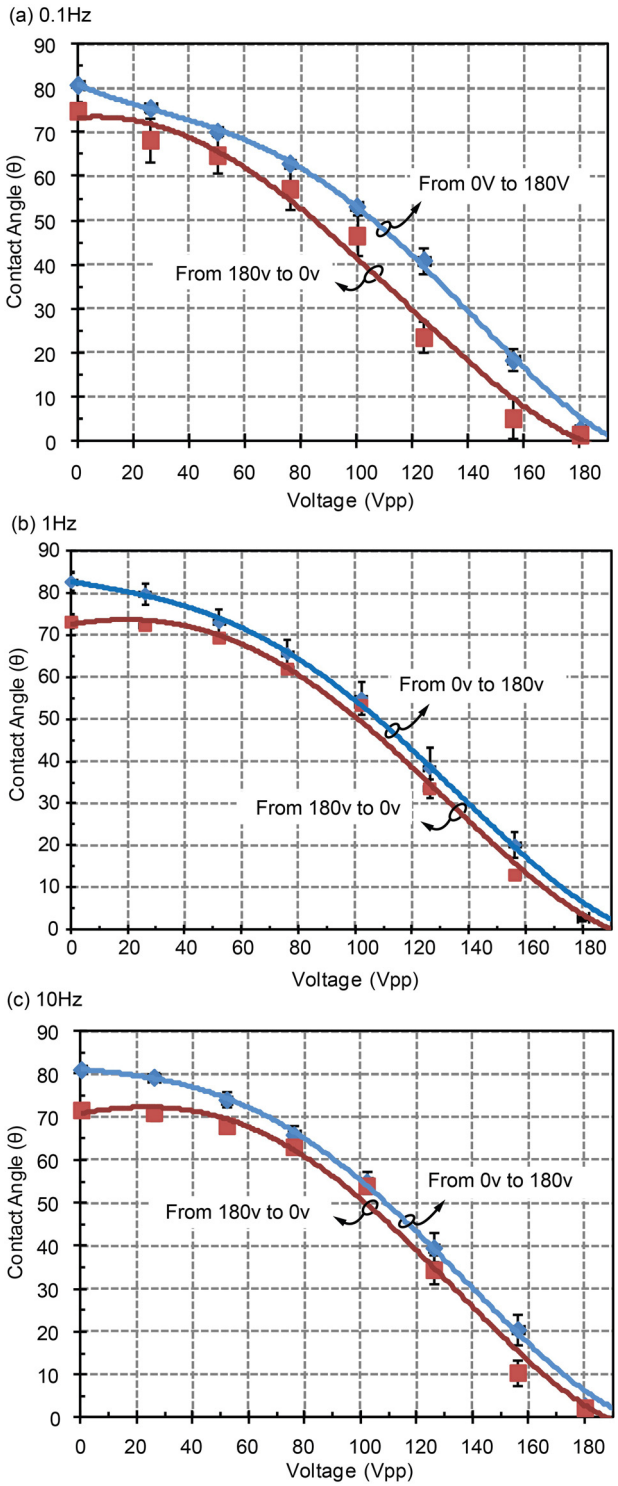


FIG. 3. Static contact angle as a function of square-wave peak-to-peak voltage (Vpp) for 0.1, 1, and 10 Hz AC voltage. Each data point was taken 2 s after the voltage was set. Three tests were performed for each data point, and statistical error bars are provided.

crystal is very viscous at ~70 cP), increasing ink surface tension, and most importantly moving to smaller and more closely spaced splitting features to reduce the required distance the ink must move during spreading or dewetting.

The minimum optical transmission of the ink film was measured to be T < 1.5% ~ 420–680 nm, for an ink film that is ~15 μm thick (see supplementary material for experimental details of the transmission measurements[24]). The ink thickness in continuous film geometry was determined using

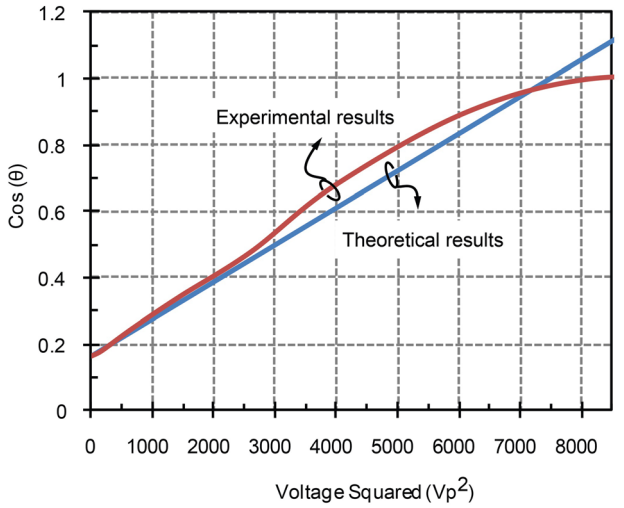


FIG. 4. Theoretical and experimental cosine of contact angle versus the square of voltage (10 Hz AC voltage).

the simple method of geometrically calculating the thickness from the dosed volume of ink and the spread area of the ink. An extensive development of dyes was not performed and the visible transmission could be much lower with further dye development since the 3 types of dyes used already suppress transmission to T < 0.2% over several 10's nm wide wavelength bands. With a maximum optical transmission of 80%, the device therefore provides excellent on/off contrast ratios of >400:1. It is important to also note that these optical properties are independent of light polarization or incident angle. Grayscale response was also measured. The ink film was first allowed to fully dewet into small droplets, then voltages increased and tuned to ~10% steps in reduction of optical transmission. The results shown in Figure 6 reveal that device is clearly capable of basic grayscale modulation, which is impressive considering that the device does not require pixelation. These results are completely unoptimized as grayscale is certainly dependent on fluid pinning at splitting features and is inhomogeneous as droplets of different sizes and spacing merge at different voltages. Optimized grayscale operation will likely utilize smaller and more numerous droplets to statistically homogenize the grayscale

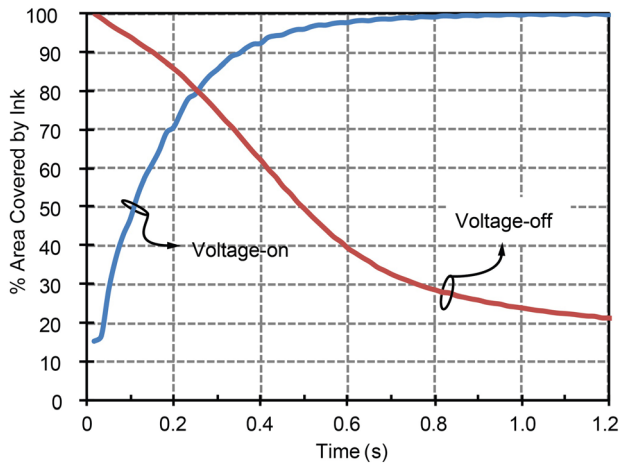


FIG. 5. Both the ink spreading vs. time with voltage on, and the dewetting vs. time when the voltage is turned off.

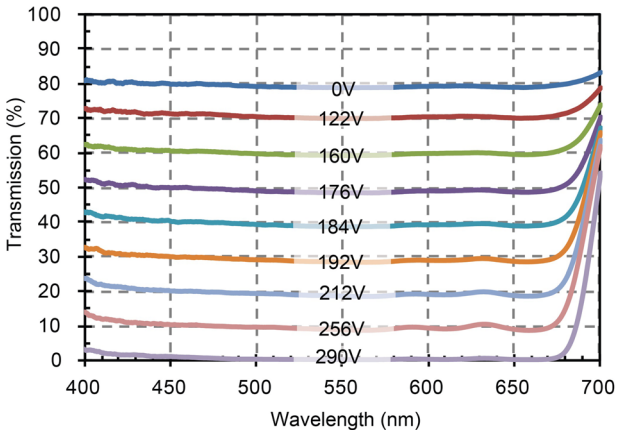


FIG. 6. Device optical transmission vs. wavelength for several voltage levels (10 Hz AC voltage, 5 cm^2 measured area). The voltage labeled for each curve is V_{pp}.

response and will seek a balance between the need for highly engineered droplet distribution, but also the need to avoid too much periodicity in droplets and splitting features which can increase both visible aliasing and optical diffraction.[29]

In conclusion, a large area optical shutter has been created using both simple yet highly effective mechanisms for creating an opaque film of ink (dielectrowetting with interdigitated electrodes) and for dewetting that film in a rapid and visually acceptable manner (splitting features for deterministic ink film breakup). The device requires only two electrical contacts and is capable of low power, grayscale, and high-contrast operation. Device behavior tracks well with theoretical models, allowing predictive design and optimization of the devices. With further development, this device could find application not served well by less transmissive technologies, with such applications including smart windows, switchable architectural glass, and segmented/symbolic large area reflective signage.

The lead author (Zhao) gratefully acknowledges partial support from the Natural Science Foundation of Jiangsu Province, China (No. BK2011752) and Research supported by Jiangsu Provincial Department of Education Scholarship for Overseas Studies, China. All the authors gratefully acknowledge partial support from the National Science Foundation (ECCS1001146 and ECCS1231668). The authors thank Dr. Russ Schwartz (Sun Chemical Corp., USA) and Fujino Nobutaka (DIC Corp., Japan) for providing fluid materials and Dr. Kenneth Dean (Gamma Dynamics Corp., USA) for providing environmental temperature and haze testing. The authors would also like to thank Glen McHale (Northumbria University) and Carl Brown (Nottingham Trent Univerisity) for early input and guidance on dielectrowetting superspreading physics and fabrication.

[1]J.-L. Chen, W. Cranton, and M. Fihn, *Handbook of Visual Display Technology* (Springer, Berlin/Heidelberg, UK, 2012, Canopus Publishing Limited, Berlin/Heidelberg/Bristol, UK, 2012).
[2]A. Giraldo, J. Aubert, N. Bergeron, E. Derckx, B. J. Feenstra, R. Massard, J. Mans, A. Slack, and P. Vermeulen, J. Soc. Inf. Disp. **18**(4), 317 (2010).
[3]J. Heikenfeld, P. Drzaic, J.-S. Yeo, and T. Koch, J. Soc. Inf. Disp. **19**(2), 129 (2011).
[4]C. Bechinger, S. Ferrere, A. Zaban, J. Sprague, and B. A. Gregg, Nature **383**(6601), 608 (1996).
[5]C. M. Lampert, Mater. Today **7**(3), 28 (2004); J. N. Yao, K. Hashimoto, and A. Fujishima, Nature **355**(6361), 624 (1992).
[6]K. Resch and G. M. Wallner, Sol. Energy Mater. Sol. Cells **93**(1), 119 (2009).
[7]D. Cupelli, F. P. Nicoletta, S. Manfredi, M. Vivacqua, P. Formoso, G. De Filpo, and G. Chidichimo, Sol. Energy Mater. Sol. Cells **93**(11), 2008 (2009).
[8]M. Saeli, C. Piccirillo, I. P. Parkin, R. Binions, and I. Ridley, Energy Build. **42**(10), 1666 (2010).
[9]R. Vergaz, J.-M. Sánchez-Pena, D. Barrios, C. Vázquez, and P. Contreras-Lallana, Sol. Energy Mater. Sol. Cells **92**(11), 1483 (2008).
[10]C. G. Granqvist, A. Azens, A. Hjelm, L. Kullman, G. A. Niklasson, D. Rönnow, M. S. Mattsson, M. Veszelei, and G. Vaivars, Sol. Energy **63**(4), 199 (1998).
[11]C. H. Lee, H. S. Lim, J. Kim, and J. H. Cho, ACS Nano **5**(9), 7397 (2011).
[12]W. Y. Lee, Y. H. Chiu, C. C. Liang, W. Y. Cheng, K. L. Lo, and Y. H. Tsai, SID Symp. Dig. Tech. Pap. **42**(1), 78 (2011).
[13]S. W. Kuo, K. L. Lo, W. Y. Cheng, H. H. Lee, Y. H. Tsai, Y. S. Ku, P. P. Cheng, P. J. Su, and J. W. Shiu, SID Symp. Dig. Tech. Pap. **42**(1), 232 (2011).
[14]G. McHale, C. V. Brown, M. I. Newton, G. G. Wells, and N. Sampara, Phys. Rev. Lett. **107**(18), 186101 (2011).
[15]G. McHale, C. V. Brown, and N. Sampara, Nat. Commun. **4**, 1605 (2013).
[16]C. V. Brown, G. G. Wells, M. I. Newton, and G. McHale, Nat. Photonics **3**(7), 403 (2009).
[17]T. B. Jones, J. Micromech. Microeng. **15**, 1184 (2005).
[18]F. Mugele and J. C. Baret, J. Phys: Condens. Matter **17**(28), R705 (2005).
[19]H. Ren and S. T. Wu, Opt. Express **16**(4), 2646 (2008).
[20]C. C. Cheng, C. A. Chang, and J. A. Yeh, Opt. Express **14**(9), 4101 (2006).
[21]S. Xu, H. Ren, Y. Liu, and S. T. Wu, Disp. Technol. J. **8**(6), 336 (2012).
[22]C. U. Murade, J. M. Oh, D. van den Ende, and F. Mugele, Opt. Express **19**(16), 15525 (2011).
[23]H. Ren, S. Xu, and S. T. Wu, Lab Chip **11**(20), 3426 (2011).
[24]See supplementary material at http://dx.doi.org/10.1063/1.4834095 for a more detailed description of the device structure, materials, fabrication, and experimental procedures.
[25]S. Chevalliot, S. Kuiper, and J. Heikenfeld, J. Adhes. Sci. Technol. **26**(12-17), 1909 (2012).
[26]A. Sharma and E. Ruckenstein, J. Colloid Interface Sci. **133**(2), 358 (1989).
[27]G. I. Taylor and D. H. Michael, J. Fluid Mech. **58**(04), 625 (1973).
[28]B. Sun and J. Heikenfeld, J. Micromech. Microeng. **18**(2), 025027 (2008).
[29]M. Hagedon, S. Yang, A. Russell, and J. Heikenfeld, Nat. Commun. **3**, 1173 (2012).
[30]K. Zhou, J. Heikenfeld, K. A. Dean, E. M. Howard, and M. R. Johnson, J. Micromech. Microeng. **19**(6), 065029 (2009).
[31]R. Igreja and C. J. Dias, Sens. Actuators, A **112**(2–3), 291 (2004).